J Fluoresc (2006) 16:555–567
DOI 10.1007/s10895-006-0091-y

ORIGINAL PAPER

Fluorescence Resonance Energy Transfer and Complex Formation Between Thiazole Orange and Various Dye-DNA Conjugates: Implications in Signaling Nucleic Acid Hybridization

W. Russ Algar · Melissa Massey · Ulrich J. Krull

Received: 25 January 2006 / Accepted: 22 March 2006 / Published online: 23 June 2006

Abstract Fluorescence resonance energy transfer (FRET) was investigated between the intercalating dye thiazole orange (TO), and the dyes Cyanine 3 (Cy3), Cyanine 5 (Cy5), Carboxytetramethyl Rhodamine (TAMRA), Iowa Black FQ (IabFQ), and Iowa Black RQ (IabRQ), which were covalently immobilized at the end of dsDNA oligonucleotides. In addition to determining that TO was an effective energy donor, FRET efficiency data obtained from fluorescence lifetime measurements indicated that TO intercalated near the middle of the 19mer oligonucleotide sequence that was used in this study. Discrepancies in FRET efficiencies obtained from intensity and lifetime measurements led to the investigation of non-fluorescent complex formation between TAMRA and modified TO. The hydrophobicity of TO was modified by the addition of either an alkyl or polyethylene glycol (PEG) side-chain to study effects of dimer and aggregate formation. It was found that at stoichiometric excesses of modified TO, fluorescence quenching of TAMRA was observed, and that this could be correlated to the hydrophobicity of a TO-chain species. The TAMRA:TO-chain association constant for the TO-alkyl system was $0.043 \pm 0.002\ M^{-1}$, while that obtained for the TO-PEG was $0.037 \pm 0.002\ M^{-1}$. From the perspective of method development for the transduction of hybridization events, we present and evaluate a variety of schemes based on energy transfer between TO and an acceptor dye, and discuss the implications of complex formation in such schemes.

Keywords Fluorescence resonance energy transfer · Thiazole orange · Förster distance · Biosensor · TAMRA

Introduction

Nucleic acid biosensor technology is being developed to provide rapid, reliable detection of pathogens and genetic diseases [1–5]. The array of technology includes piezoelectric [3, 6], electrochemical [7, 8], and optical methodologies [5, 9–11]. In many cases the ultimate goal is to create a sensitive, selective, and reusable field-deployable device for rapid diagnostics. Fluorescence based biosensor strategies are often very sensitive in that they can be designed to concurrently offer significant signal while also minimizing background (noise). In particular, fluorescence resonance energy transfer (FRET) has been used to develop analytical methods that are suitable for investigation of the extent of selective binding by observation of associated proximity effects on fluorescence intensity and lifetimes. For example, Molecular Beacons represent a technology that uses FRET to develop an analytical signal as well as to suppress background fluorescence intensity. This approach also offers the significant advantage that target molecules do not need to be fluorescently labelled in a separate step. Unfortunately, the sequence selectivity of molecular beacons is limited due to the short stem sequences that are required for function. In contrast, we are investigating FRET-based transduction strategies in which an intercalating dye that can interact with fluorophore or quencher end-labelled DNA could signal hybridization events while maintaining good selectivity. In some of the strategies presented, labeling of target is also avoided.

The authors wish it to be known that they have participated equally in the experiments and preparation of this manuscript and should, in their opinion, be considered joint first authors.

W. R. Algar · M. Massey · U. J. Krull (✉)
Chemical Sensors Group, Department of Chemical & Physical Sciences, University of Toronto at Mississauga, South Building, Room 2035, 3359 Mississauga Road North, Mississauga, Ontario, L5L 1C6 Canada
e-mail: ukrull@utm.utoronto.ca

Intercalators are a class of fluorescent dyes that associate with double-stranded DNA (dsDNA) and can serve to provide fluorescence changes that can be used as an analytical signal to determine hybridization. Ethidium bromide (EB) is one of the best known intercalators that is used in the detection of dsDNA [12]. EB is just one of many known fluorescent intercalating dyes, and does not offer optimal analytical performance as a marker for detection of dsDNA structure due to its relatively low fluorescence enhancement upon binding and relatively low molar absorptivity. Thiazole orange (TO) is another dye that has been used as an intercalative transduction agent in nucleic acid hybridization assays. TO is a non-planar chromophore composed of a benzothiazole derivative and a quinolinium ring linked *via* a monomethine bridge. TO has been reported to provide anywhere from a 50- to a 18 900-fold fluorescence enhancement upon dsDNA binding [13, 14]. Regardless of whether the enhancement is in the upper or lower limit of this range, it is a substantial improvement in comparison to the emission from EB [15, 16]. It is worth noting that differing experimental conditions including nucleotide sequence [14, 17] can influence the degree of fluorescence enhancement that is observed. The increase in quantum efficiency of TO upon intercalation results from the restriction of rotation around the monomethine bridge connecting the benzothiazole and quinolinium heterocycles of the dye. Both the benzothiazole and quinolinium rings adapt to the propeller twist of the base pairs, while a charge symmetry is created through resonance by the two nitrogen atoms present in the molecule [18]. In free solution, the monomethine bridge has a low energy barrier to rotation and hence is prone to relax non-radiatively from an electronically excited state [18]. The non-radiative decay rate depends on twist angle, and consequently quantum yield depends on the solvent viscosity/rigidity of the surrounding media [19]. Thus, TO is weakly fluorescent in solution and highly fluorescent in viscous or rigid media, making it an excellent choice as an intercalator that can indicate DNA hybridization.

Selective transduction of dsDNA structure by use of a fluorescent intercalating dye is highly advantageous in nucleic acid biosensor design in comparison to an indirect method that only indicates the presence of a fluorescently labelled target. An intercalating dye such as TO is necessary in this respect due to its strong dependence on stable hybrid formation and low fluorescence in the presence of single-stranded DNA (ssDNA). However, intercalating dye not associated with dsDNA still has a finite quantum yield. It may be possible to further decrease background signal and thereby enhance signal-to-noise in the presence of ssDNA by relying on a FRET strategy. The presence of a fluorophore- or quencher-labelled sequence offers the possibility of two sensitivity enhancement strategies: (1) incorporating a quencher-labelled sequence to effectively eliminate background fluorescence; or (2) incorporating a fluorescent acceptor to allow for ratiometric quantification and greater confidence in observed signals.

In this new work, we present the preliminary stages of development of an intercalator-based FRET strategy for signaling nucleic acid hybridization events. This paper does not report a method in itself, but rather the first step in developing a methodology ultimately intended for use in a nucleic acid biosensor. Our interest at present lies in characterizing the energy transfer, physical behaviour, and interactions between the dye species involved in the FRET-based transduction strategies we propose. In light of this objective, we take a minimalist approach to the systems studied. For example, we use monomeric TO dye modified with an alkyl or a polyethylene glycol (PEG) side-chain as a model system. In this work, the side-chain modification allows control over hydrophobicity, but more generally allows the monomeric TO to be covalently tethered to a probe oligonucleotide, as previously described and characterized by our group [20, 21]. This latter feature has not been exploited at present so as to isolate the physical behaviour of the dye molecules, without restrictions and perturbations of the tethering process superimposed. The study remains of practical importance because the use of a tethered intercalator, though advantageous, is neither commonplace nor required for effective biosensor design. Indeed, we find that the spectroscopy of the TO-FRET-systems studied are complicated by the potential for hydrophobicity and stoichiometrically driven non-fluorescent complex formation with an acceptor dye. In addition to characterizing complex formation, we demonstrate energy transfer from TO to various dye-dsDNA conjugates and have determined the corresponding Förster distances.

A second interesting aspect of this work is the use of monomeric TO which, when compared to the array of work using dimeric TO derivatives [for example, 22–25], is much less studied. Monomeric TO is advantageous from a biosensor perspective because it shows much less sequence selectivity for intercalation than dimeric TOTO, and also because the TO-TO bridge in the dimer occupies the site most effectively used for attachment of a tether [26]. In addition, TOTO binds less reversibly to dsDNA which may hinder the use of TOTO in a reusable biosensor construct, while also exhibiting a smaller dsDNA/ssDNA fluorescence ratio [12, 27]. Although FRET between dimeric TOTO species and many other heterodimeric intercalators has been reported [28–36], we believe that this report is the first instance of FRET between an intercalator and a distinct, extrinsic fluorophore (in this work *extrinsic* refers to any non-intercalating dye conjugated to either terminus of an oligonucleotide).

Experimental

Reagents

All chemicals were reagent grade or better and used without further purification. Reagents used for thiazole orange synthesis (methyl iodide, 2-(Methylthio)benzothiazole, 4-Methylquinoline, Triethylamine, Triethylene glycol monochlorohydrin, Sodium iodide) were from the Aldrich Chemical Company (Milwaukee, WI, USA). Oligonucleotide solutions were prepared in 1 × PBS buffer; buffers were prepared with double-distilled water and subsequently autoclaved. Buffer salts (sodium chloride, dibasic sodium phosphate) were obtained from Aldrich. Purified water with a specific resistance no less than 18 MΩ-cm (Milli-Q cartridge purification system, Millipore Corporation, Mississauga, ON, Canada) was used in octanol–water partitioning experiments, and 99% octanol was obtained from Sigma (Oakville, ON, Canada).

Synthesis of thiazole orange

The synthesis of thiazole orange with various side-chains was based upon the methods of Brooker *et al*. [37, 38] and Carreon *et al*. [39]. The quinolinium compounds were synthesized by treating 4-Methylquinoline (lepidine) with 3 equivalents of the appropriate iodo-functionalized side-chain in refluxing toluene followed by solvent extraction in CH_2Cl_2/H_2O, dried with $CaCl_2$, and subsequently recrystallized from acetone. The side-chain functionalized quinolinium compounds were then condensed with the benzothiazole derivative in the presence of triethylamine in ethanol to give the dye species. The dye species were recrystallized from $MeOH/H_2O$. This species is referred to as TO-alkyl.

For the triethylene-glycol side-chain quinolinium derivative, triethylene glycol monochlorohydrin was converted to triethylene glycol monoiodohydrin according to the method of Koizumi *et al*. [40] (not shown). This species is referred to as TO-PEG. The synthetic schemes for both the TO-PEG and TO-alkyl dyes are shown in Fig. 1.

Dye labelled oligonucleotides

The oligonucleotide sequences in Table 1 were obtained from Integrated DNA Technologies (Coralville, IA, USA) and dissolved in 1 × PBS buffer at pH 7.0. The base sequence corresponds to the SMN1 gene fragment used in oligonucleotide diagnostics for spinal muscular atrophy [5]. All subsequent dilutions were also prepared with 1 × PBS buffer. Solutions containing a 1:1 ratio of probe and target oligonucleotides were heated at 95°C for 5 min and allowed to slowly cool to room temperature to generate dsDNA.

Oligonucleotide solutions used in the measurement of spectral properties and energy transfer were 0.5 μM in dsDNA (i.e. 1.0 μM in total oligonucleotide). Oligonucleotide solutions used to evaluate the potential for background suppression and ratiometric measurements via FRET were prepared as follows: ssDNA was mixed with TO-PEG stock solution and PBS buffer to produce a solution 1.0 μM in each, and let stand for 30 min prior to analysis; 1.0 μM dsDNA solutions (2.0 μM total oligonucleotide) were prepared as described above, mixed with an equivalent of TO-PEG, and let stand 30 min.

Association studies

Solutions used in the study of the association of TO-chain and TAMRA labelled oligonucleotide were prepared by mixing buffered solutions of free side-chain modified TO and either ssDNA or dsDNA. The solutions were then mixed for approximately 1 hr. Stock solutions of side-chain modified TO were 100 and 200 μM for the polyethylene glycol and alkyl modified dyes, respectively. The former was entirely aqueous, and the latter was dissolved in a 1:1 water:methanol solution. Oligonucleotide solutions for analysis were in the concentration range of 0.25–0.50 μM.

Instruments

Ultraviolet-visible absorption spectra were collected using a Bichrom Ltd. (Cambridge, UK) Libra S22 spectrometer and a Hewlett Packard 8452A Diode-Array Spectrometer (Hewlett Packard Corporation, Palo Alto, CA). Solution phase fluorescence spectra were collected using a QuantaMaster PTI Spectrofluorimeter and Felix Software (Photon Technology International, Lawrenceville, NJ, USA). Moisture content measurements of dry solvents were determined using an AquaStar® Karl Fischer Titrator (EMD Chemicals Inc., Gibbstown, New Jersey, USA) which provided a readout of H_2O concentration in parts-per-million.

Fluorescence lifetime data was obtained with a time correlated single photon counter (constructed in-house), driven by a 520 nm femtosecond laser (pulse duration: 200 fs, repetition rate: 15 MHz, bandwidth: 3 nm, mean power: 30 mW).

Spectral data, lifetime, and forster distance calculations

The donor–acceptor distance-efficiency relationship is given by Eq. (1), where R_o is the Förster distance, R is the donor–acceptor separation, and E is the energy transfer efficiency. The Förster distance (Eq. (2)) is a characteristic of a donor–acceptor pair, and depends on factors including refractive index of the surrounding medium, n, the donor quantum yield, Φ_D, the relative orientation between donor emission and acceptor absorption dipoles, and the degree of spectral

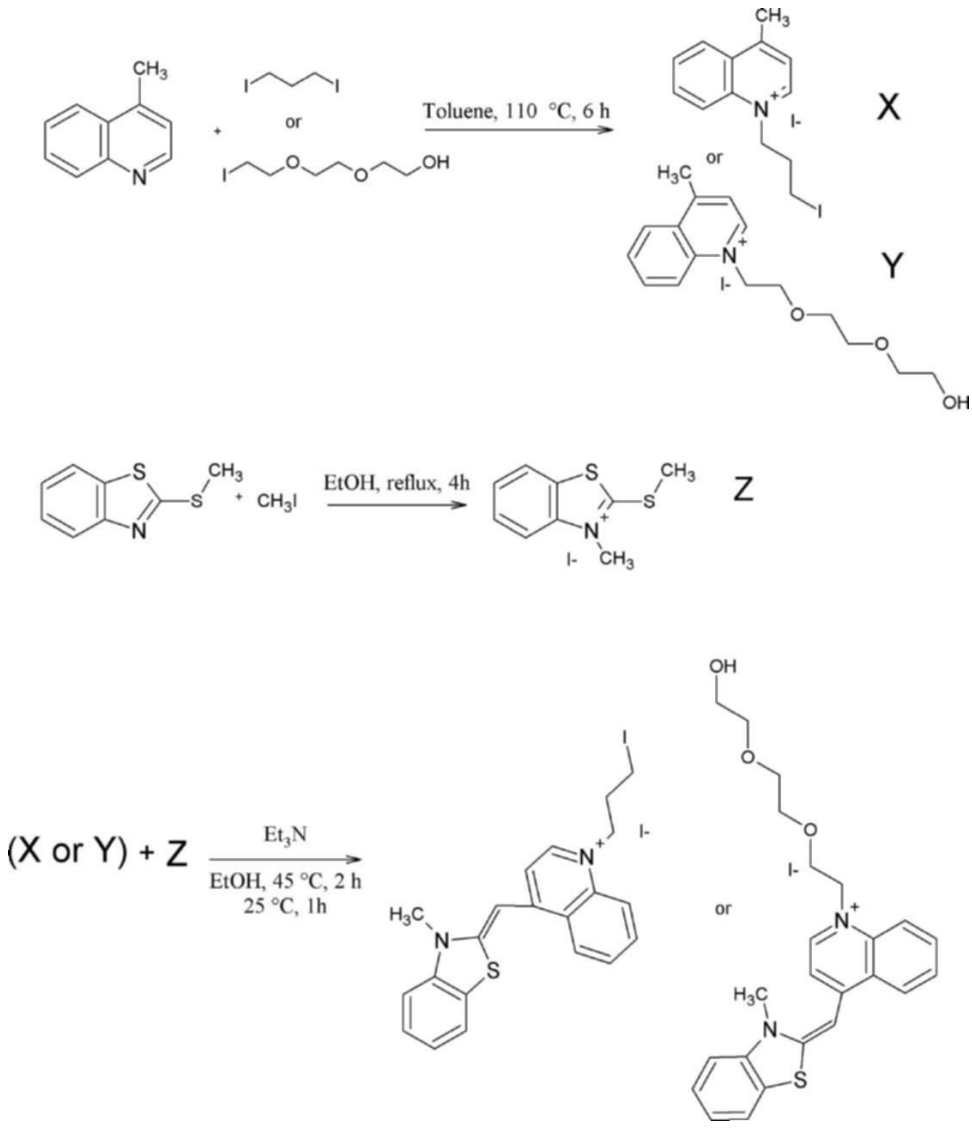

Fig. 1 Synthetic scheme for the preparation of thiazole orange dye and the attachment of different side-chains

resonance between the two species [41]. These latter two parameters are described by the orientation factor, κ^2, and spectral overlap integral, J, respectively. The spectral overlap integral (Eq. (3)) is a function of the fluorescence intensity of the donor, F_D, and molar absorptivity of acceptor, ε_A, as a function of wavelength, λ, normalized against the total donor emission [41]. In the case of donor and acceptor molecules that are free to sample all orientations, the orientation factor assumes a value of $\kappa^2 = 2/3$.

$$E = \frac{R_o^6}{R_o^6 + R^6} \tag{1}$$

$$R_o^6 = 8.79 \times 10^{-28}\,\text{mol} \times (n^{-4}\kappa^2 \Phi_D J) \tag{2}$$

$$J = \frac{\int F_D(\lambda)\varepsilon_A(\lambda)\lambda^4 d\lambda}{\int F_D(\lambda) d\lambda}. \tag{3}$$

Ultraviolet-visible absorption and fluorescence emission spectra were obtained with 3 and 0.5 μM solutions of oligonucleotide, respectively. From the spectra obtained, the integrands in Eq. (3) were calculated at 0.5 nm increments and integrated numerically to determine the spectral overlap. The refractive index and orientation factor terms in Eq. (2) were taken as $n = 1.43$ and $\kappa^2 = 2/3$, corresponding to the refractive index of buffer and non-restricted dye motion. The excitation wavelength for TO was set to be 507 nm.

Quantum yield values for fluorescent dyes were determined relative to fluorescein dye in sodium borate buffer fixed at pH 9.5. The quantum yield of fluorescein under these conditions is known to be 0.93 [42], and the quantum

Table 1 Oligonucleotide sequences and labels used in FRET experiments

Probe	5′-ATT TTG TCT GAA ACC CTG T-Cy3/TAMRA-3′
Target	5′-Cy5/IabRQ/IabFQ-A CAG GGT TTC AGA CAA AAT-3′
Abbreviations	
Cy3	N,N′-(diisopropyl)-tetramethylindocarbocyanine
Cy5	N,N-(diisopropyl)-tetramethylindodicarbocyanine
TAMRA	Carboxytetramethylrhodamine
IabRQ	Iowa Black RQ
IabFQ	Iowa Black FQ
TO[a]	Thiazole orange

Labelled target sequences were hybridized with unlabelled probe sequences to generate dsDNA, and vice versa.

[a]TO is not covalently tethered to either terminus of the oligonucleotide.

yield, Φ, of other dyes were determined as a ratio (Eq. (4)) of their integrated emission, $\int F d\lambda$, corrected for different molar absorptivity coefficients, ε, at the wavelength of excitation. Fluorescein was excited at 490 nm.

$$\frac{\int F d\lambda}{\int F_{\text{ref}} d\lambda} = \frac{\varepsilon}{\varepsilon_{\text{ref}}} \frac{\Phi}{\Phi_{\text{ref}}}. \tag{4}$$

Lifetime measurements were made with 3 μM solutions and were calculated from fluorescence decay curves using SPCImage software (Version 2,7,27,38,0) from Becker & Hickl GmbH (Berlin, Germany). The best fit was obtained by minimizing the chi-squared value. It should be noted that the chi-squared value provided by the software is not normalized.

Octanol–water partition experiments

Standard aqueous solutions of PEG (3.6 μM) and alkyl (3.4 μM) modified TO were prepared. An equal volume of octanol was added to an aliquot of aqueous standards. The mixtures were slowly stirred for approximately 18 hrs. The peak absorbance for the aqueous phases were compared to that of the standard solutions and used to determine the concentration of the TO species in each phase.

Results and discussion

Energy transfer between thiazole orange and an extrinsic dye label

Thiazole orange and other intercalating dyes are particularly useful in that their fluorescence intensity is dependent on selective partitioning of the dye into dsDNA. In contrast, emission from Cy3 or TAMRA cannot effectively differentiate between ssDNA and dsDNA without some external reference or calibration [43]. As a first step towards a FRET-based strategy employing TO, we have demonstrated that TO can participate in energy transfer with an extrinsic dye (i.e. not an intercalator) that is covalently attached to the terminus of a DNA oligonucleotide.

In the presence of an extrinsic label, the fluorescence of intercalated TO-PEG was found to be significantly quenched. The fluorescence spectra in Fig. 2 show quenching efficiencies of 97%, 88%, 88%, 86%, and 80% for TO-PEG with ds-DNA conjugates of Cy3, TAMRA, IabFQ, Cy5, and IabRQ as energy acceptors. The Förster distances for these TO-acceptor pairs were experimentally determined from their respective emission and absorption profiles and are tabulated in Table 2. These quenching efficiencies roughly mirror the trend observed in the spectral overlap between TO and the various acceptors. In the case of Cy3 and TAMRA acceptors, an increase in emission was also observed. This is thought to be emission sensitized by energy transfer from TO to Cy3 or TAMRA. A slight red-shift of the emission max was also observed with Cy3.

Fluorescence lifetime data suggests that the mechanism of TO quenching includes an energy transfer process for the IabFQ, IabRQ, and Cy5 acceptor species. The measured fluorescence lifetimes for intercalated TO in the absence of an acceptor, and in the presence of IabFQ, IabRQ, or Cy5 are tabulated in Table 3. As with steady-state quenching efficiency, the decrease in lifetime mirrors the decrease in spectral overlap between the dye-acceptor pairs. Unfortunately, the lifetime changes for TO in the presence of Cy3 and TAMRA could not be determined due to the limited spectral resolution of the available instrumentation. The intense fluorescence of these two dyes at the excitation wavelength of TO prevented resolution of TO fluorescence. It was found that the fluorescence lifetimes of Cy3 and TAMRA in ds-DNA were 2.0 and 4.2 ns, respectively, and this prevented time-based resolution with respect to TO fluorescence. The fluorescence of Cy5-dsDNA was sufficiently low as not to interfere with the measurement of TO fluorescence at the excitation wavelength (520 nm).

Assuming that, on average, TO intercalates at the same position in the dsDNA regardless of extrinsic label, the correspondence between spectral overlap and both quenching efficiency and TO lifetime suggests a Förster type energy transfer process for the TO donor with the IabFQ, IabRQ, and Cy5 acceptors. Calculating the donor–acceptor distance, R, based on the quenching efficiencies and TO fluorescence lifetimes (Eq. (5)) yields the data summarized in Table 4. In Eq. (5), the subscripts DA and D refer to donor (TO) emission in the presence of acceptor and donor emission in the absence of acceptor, respectively. F_{DA} and F_{A} are

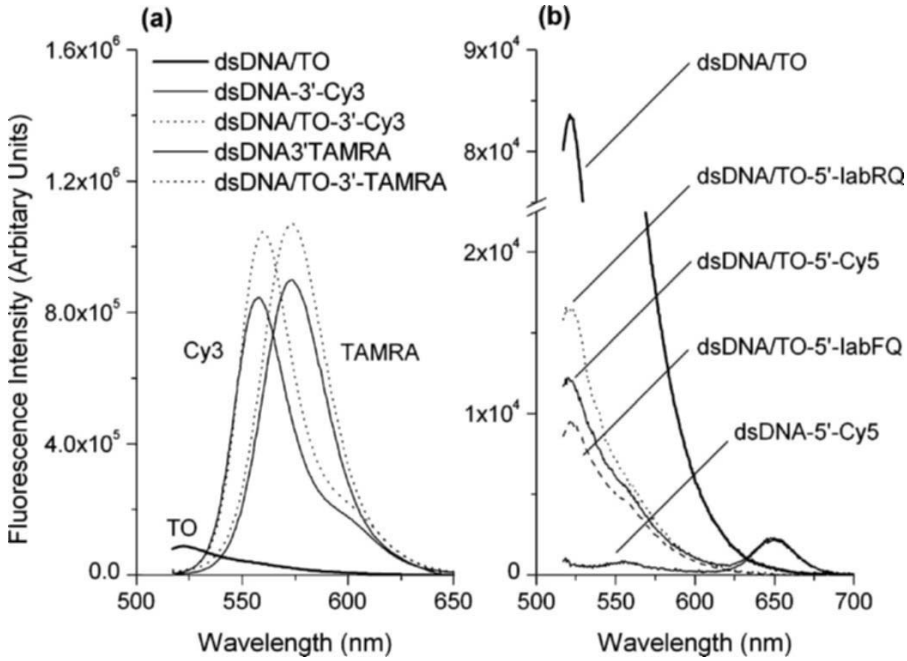

Fig. 2 Fluorescence spectra (a) showing quenching of TO fluorescence by Cy3 and TAMRA. Note the changes in the emission profiles of Cy3 and TAMRA. Cy3 shows the largest quenching of TO as well as increased emission and a slight red-shift; TAMRA shows similar effects. Quenching of TO fluorescence was also observed with IabFQ, Cy5, and IabRQ in (b). Note that there was no appreciable change in Cy5 emission. All solutions are 0.5 μM in both labelled dsDNA and TO-PEG (where applicable)

similarly related to fluorescence intensity; the lifetime of TO is denoted by τ.

$$E = 1 - \frac{(F_{DA} - F_A)}{F_D} = 1 - \frac{\tau_{DA}}{\tau_D} = \frac{R_o^6}{R_o^6 + R^6}. \quad (5)$$

Examining the data in Table 4, it is immediately obvious that the quenching and lifetime data do not yield the same energy transfer efficiencies. We hypothesize that this results from the formation of a non-fluorescent complex between TO and the various acceptor dyes. A second quenching pathway resulting from formation of such a complex, superimposed on the FRET-based quenching pathway is consistent with the discrepancy in Table 4. The fluorescence lifetime is insensitive to non-fluorescent complex formation and thus represents the true FRET efficiency. The quenching efficiency observed in steady state measurements is the net effect of these two pathways. The lifetime calculated donor–acceptor distances correspond to a position approximately in the center of the 19-base pair oligonucleotide sequence, which does reflect the most stable position for TO to intercalate (considering the ensemble average). This lends additional confidence to the lifetime data and suggests that complex formation is able to compete with intercalation to some extent. In terms of method development for biosensor design, this highlights a potential source of spurious signals which could plague an assay. Thus an understanding of the physical interaction between the donor and the acceptor is critical, and the subject of the discussion in a latter section.

The orientation factor, κ^2, is often a point of difficulty in the study of systems with limited mobility [44]. Although the acceptor molecules in this work have a large degree of rotational freedom, it is not necessarily the case that $\kappa^2 = 2/3$ since TO is essentially immobilized within the double helix (for example, Shins *et al*. have studied dipole orientation in the TOTO-DNA system [45]). Furthermore, if these acceptor dyes have differing tendencies to associate or aggregate with DNA, then the orientation factor becomes both a function

Table 2 Fluorescence and energy transfer data calculated from experimental data for various TO-acceptor pairs

Acceptor	TO quantum yield, Φ	Spectral overlap, J (10^{-10} cm^6)	Förster distance, R_o (nm)
TO	0.011 ± 0.002	0.76 ± 0.20	2.3 ± 0.7
Cy3		5.2 ± 1.1	3.2 ± 0.9
TAMRA		3.7 ± 0.8	3.0 ± 0.8
IabFQ		2.4 ± 0.5	2.8 ± 0.8
Cy5		1.6 ± 0.4	2.6 ± 0.8
IabRQ		0.6 ± 0.2	2.2 ± 0.8

Note. The spectral overlap integral for each pair is given separately to allow calculation of the Förster distance for any index of refraction and orientation. The listed Förster distance employs values of 1.48 and 2/3 for the refractive index and orientation factor, respectively.

Table 3 Fluorescence lifetimes measured for TO intercalated in unlabelled, IabFQ-, IabRQ-, and Cy5-labelled dsDNA conjugates

Acceptor dye	Lifetime (ns)
(none)	2.6
IabFQ	1.8
IabRQ	2.2
Cy5	2.0

Table 4 Energy transfer efficiencies and TO-acceptor distances deduced from TO fluorescence quenching efficiency and changes in TO fluorescence lifetime

Acceptor	Quenching		Lifetime	
	Efficiency, E	Distance, R (nm)	Efficiency, E	Distance, R (nm)
Cy3	0.97	1.8	—	—
TAMRA	0.88	2.1	—	—
IabFQ	0.88	2.0	0.31	3.2
Cy5	0.86	1.9	0.23	3.2
IabRQ	0.80	1.7	0.15	2.9
Average (± standard deviation)	—	1.9 (± 0.2)	—	3.1 (± 0.2)
Approximate number of bases from extrinsic dye labelled terminus	—	5–6	—	9–10

of the degrees of freedom associated with the linkage, and the dye-DNA interactions. An estimation of these effects is beyond the scope of this work, and thus it is unclear if the observed of standard deviation of 0.2 nm for the calculated R values represents true variability in the TO-acceptor distance, variability in the orientation factor, or possibly contributions from both of these two effects. Nonetheless, the approximation of $\kappa^2 = 2/3$ seems to be reasonable in this particular case.

Potential FRET-based transduction strategies for DNA hybridization

We initially suggested two possible strategies for improving signaling of hybridization events through the use of TO and FRET: (1) background suppression through the use of a dark quencher; and (2) ratiometric measurements with the use of a second fluorophore. With respect to (1), Fig. 3 shows the peak emission intensities for various permutations of TO with ssDNA and dsDNA, as both IabFQ-labelled or unlabelled sequences. It is immediately obvious that TO has significant background fluorescence in the presence of ssDNA, albeit considerably less than that of intercalated TO. However, note that TO in the presence of IabFQ-labelled ssDNA shows an extremely low fluorescence which is comparable to isolated TO dye in solution. The quenching of non-intercalated TO via FRET is a result of an association of the positively charged TO with the polyanionic probe sequence. This association is also largely responsible for the fluorescence observed from non-intercalated TO (Fig. 3). Note that the emission from TO in the absence of DNA is only 4% of that observed in the presence of non-labelled ssDNA, suggesting that the association partially restricts rotation about the monomethine bridge in TO. In Fig. 4 we compare the anticipated signal-to-noise (S/N) ratios for various hypothetical assay schemes based on the data in Fig. 3. The 'noise' is defined as the TO fluorescence in the absence of probe (P)/target (T) duplex; the 'signal' is defined as that in the presence of P/T duplex. These schemes are as follows:

1. The typical assay in which the enhancement of TO fluorescence upon intercalation is used to detect P/T hybridization events. The anticipated S/N ratio is 21.
2. A modification of the typical assay which uses IabFQ-labelled P to suppress background fluorescence from non-intercalated TO prior to P/T hybridization. Despite the reduction in intercalated TO fluorescence due to the IabFQ, the much reduced fluorescence from non-intercalated TO leads to an anticipated S/N ratio increase to a value of 76.
3. This is a competitive hybridization scheme in which a IabFQ labelled sequence (D) is displaced from the probe sequence by the target sequence. Due to the relatively large TO fluorescence expected from the IabFQ-D/P hybrid with respect to the T/P hybrid, the anticipated S/N ratio is poor, having a value of 6.
4. This strategy requires that TO is initially associated with IabFQ-labelled ssDNA and subsequently intercalates in

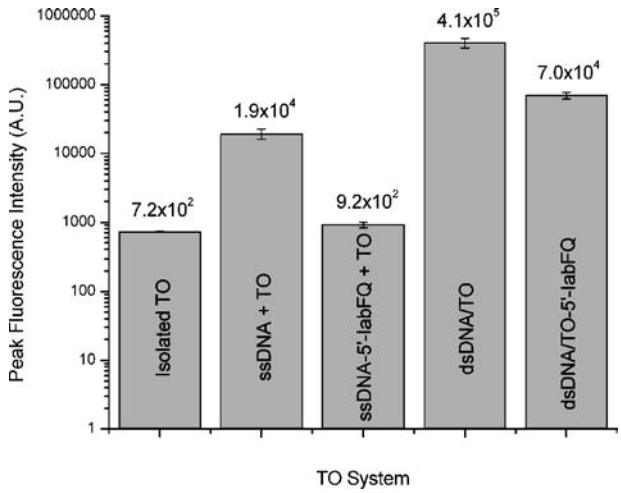

Fig. 3 Peak fluorescence intensities (measured at 520 nm) for various solutions containing 1 μM of TO. The fluorescence intensity is expressed as a logarithmic scale. Note the comparatively low fluorescence of the TO in the absence of DNA or in the presence of ssDNA labelled with IabFQ

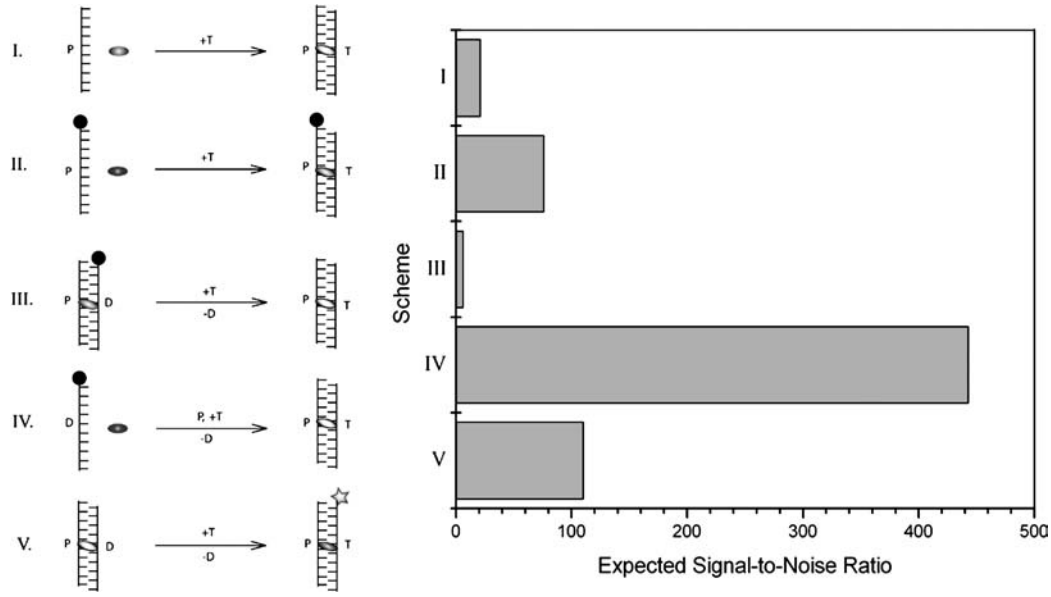

Fig. 4 Anticipated signal-to-noise ratios for various proposed probe/target hybrid detection schemes. Refer to the main text for a description of schemes. The values shown at right are calculated based on the data presented in Figs. 2 and 4. Legend: (P) probe; (T) target; (D) displaced sequence; (●) IabFQ; (○) TO; (☆) TAMRA. The shading of each symbol qualitatively represents its emission intensity

P/T duplex, ideally yielding a S/N ratio of 443. This could be referred to as a competitive association scheme since it would not be possible to prevent TO from associating with single-stranded P instead of D. If there was an equal tendency for TO to associate with P and D, the expected S/N ratio decreases to 40.

Although it may seem counterintuitive, scheme II appears to be a simple means by which to enhance the sensitivity of a hybridization assay with TO by almost a factor of 4. While scheme IV offers a much larger potential increase in sensitivity (ca. 22-fold), it is not readily implemented. Solutions of TO were prepared with different ratios of unlabelled and IabFQ-labelled sequences, and the TO fluorescence measured. The results indicated that there is no preference for TO association with the IabFQ-labelled sequence (data not shown). Clearly a biosensor strategy employing scheme IV will not be easily achieved, although it may be possible with elaborate molecular 'switch' chemistry.

Considering ratiometric measurements as described in (2), the use of a competitive hybridization scheme employing TAMRA labelled target could potentially increase sensitivity by a factor of five. As shown as scheme V in Fig. 4, an initial P/D hybrid could be displaced in favour of a TAMRA-T/P hybrid. Comparing the ratio of fluorescence intensities at the peak emission wavelengths for each dye (roughly 520 and 570 nm for TO and TAMRA respectively) before and after the displacement events would ideally yield a S/N ratio of 110. This estimate is based on the change in emission from TAMRA as dsDNA conjugate with and without intercalated TO. In practice, the TAMRA would be weakly associated with ssDNA prior to hybridization. We have previously reported that the quantum yield of TAMRA increases by 28% upon hybridization [43], and considering this additional increase in the fluorescence at 570 nm, a S/N ratio of 132 could be approached. Although one could imagine a similar scheme using Cy3 as an acceptor, a 40% reduction in the quantum yield of Cy3 accompanies hybridization [43], thus counteracting the TO-FRET sensitized increase in fluorescence. Nonetheless, TAMRA appears to be an excellent candidate for such a transduction strategy.

Although labeling of target is still required in scheme V, the use TO and FRET in conjunction with an extrinsic dye is still advantageous in practical application. Many optical biosensor devices use surface sensitive evanescent wave excitation. When only labelled target is employed, non-specific adsorption will yield a fluorescent signal which is indistinguishable from hybrid formation. With scheme V, non-specific adsorption could be differentiated since it is less likely to decrease the TO emission signal via FRET. The effectiveness of this scheme would be maximized by using extrinsic and intercalator dyes with absorption coefficients and quantum yields of similar magnitudes.

Non-fluorescent complex formation between modified TO and TAMRA

The formation of non-fluorescent ground-state complexes between dyes, including rhodamines and cyanines, has been previously reported [46–51]. In each case, it is believed that hydrophobic interactions (in an aqueous environment)

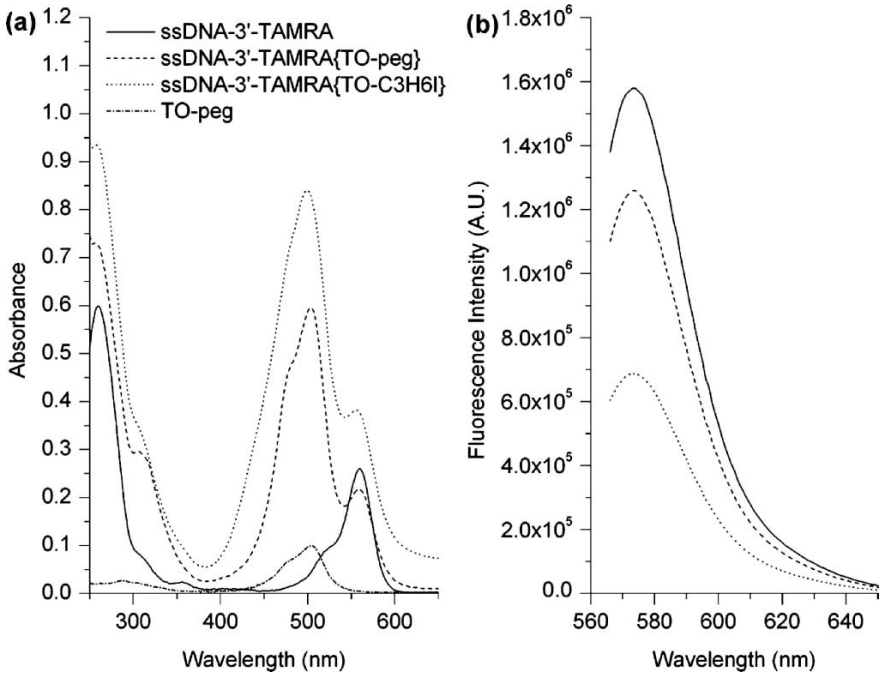

Fig. 5 Absorption and fluorescence spectra for TAMRA labelled ssDNA in the absence and presence of TO. As the TO is made more hydrophobic by changing the nature of the side chain, complex formation appeared to occur to a greater extent. This is suggested by changes in the absorption spectrum and an increase in fluorescence quenching with increasing hydrophobicity. (a) Absorption profiles for 3.0 μM TAMRA-labelled ssDNA in the absence and presence of ten equivalents of TO-PEG or TO-alkyl. The absorption profile of a stoichiometric equivalent of TO is shown for reference. (b) The fluorescence of 0.4 μM TAMRA is quenched by the formation of a ground-state complex with ten equivalents of TO-PEG and TO-alkyl. Fluorescence is excited at 556 nm, where TAMRA shows strong absorption but TO is only very weakly absorbing

are the driving force behind complex formation. TO was modified in these experiments with an alkyl chain or PEG, providing different hydrophobicities. Fluorescence and absorption spectra for TAMRA labelled ssDNA with a 10-fold excess of modified TO are shown in Fig. 5. The spectra show increased fluorescence quenching of TAMRA and a change in absorption profile in the presence of a 10-fold excess of TO. The effect was also observed to increase as the TO was made more hydrophobic by replacing the PEG side-chain with an alkyl side-chain, thus supporting the hypothesis of the role of complex formation. The octanol–water partition coefficients, K_{ow}, were determined to be 0.10 ± 0.02 and 0.87 ± 0.04 for the TO-PEG and TO-alkyl systems respectively, confirming the greater hydrophobicity of the derivative with the alkyl side-chain. Note that the absorption profiles for TO-alkyl and TO-PEG show no significant differences. The distinctly different absorption profiles in Fig. 5 are very likely due to different extents of complex formation.

Static quenching by the formation of a non-fluorescent complex (also known as quenching by preassociation) is known to follow the relationship described by Eq. (6), where F_o and F are the fluorescence intensities of the unquenched and quenched states, K is the association constant, and $[Q]$ is the concentration of quencher. This equation is generally applied to quenching by preassociation [52] and should not be confused with the isomorphous Stern-Volmer equation for dynamic quenching.

$$\frac{F_o}{F} = 1 + K\,[Q]\,. \tag{6}$$

As shown in Fig. 6, the TAMRA fluorescence of different TO:TAMRA-ssDNA conjugate ratios were measured and yields the linear relationship defined by Eq. (6) at stoichiometric excesses of TO. A greater extent of quenching was observed with the alkyl side-chain versus the PEG side-chain. The association constants were 0.043 ± 0.002 M^{-1} and 0.037 ± 0.002 M^{-1} respectively. Once again, this suggests a hydrophobic aspect to the TO-TAMRA interactions. Deviations from linearity existed at TO-TAMRA-ssDNA ratios that were lower than 2:1 indicating that the TO species was not quenching the TAMRA fluorescence as effectively as at higher TO-TAMRA ratios. This may have been due to a weak association with the TAMRA and/or the polyanionic backbone of the DNA. Recall that both TO species are positively charged and that there may also be hydrophobic interactions between the TO and the nucleobases. It is possible that the weak association may have served to decrease the collisional deactivation rates in the local environment of the TAMRA, thus increasing the observed TAMRA fluorescence. Similar changes in local environment are thought

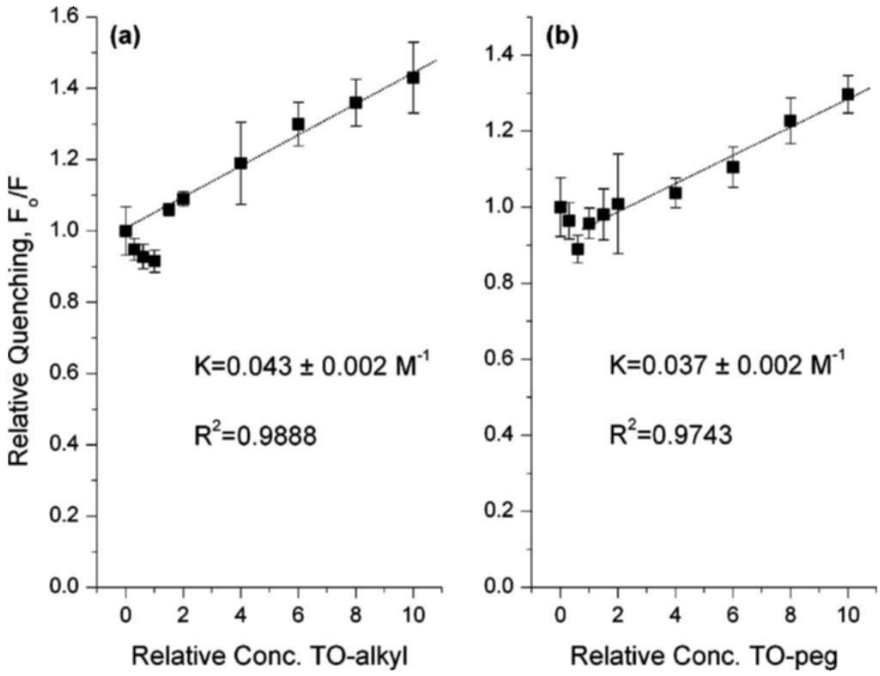

Fig. 6 (a) Quenching of TAMRA-ssDNA fluorescence as a function of the relative concentration of TO-alkyl. The linear fit is applied to ratios beyond 2:1 with the slope representing the TO-TAMRA association constant, K. The linear correlation coefficient is denoted by R^2. (b) Analogous data for the association and quenching of TO-PEG with TAMRA-ssDNA. The linear fit is applied beyond ratios of 1:1. The concentration of TAMRA-ssDNA in each case is 0.4 μM

to lead to an increase in TAMRA fluorescence when going from ssDNA to dsDNA [43].

The interaction of TO with TAMRA-dsDNA conjugates was also investigated, and Fig. 7 shows similar quenching to that observed for TAMRA-ssDNA conjugates at stoichiometric excesses of TO-PEG. The concentration dependent fluorescence of TO with respect to unlabelled dsDNA is also shown in Fig. 7. In the absence of TAMRA, TO fluorescence increased linearly with TO concentration until stoichiometric excess was reached. Even so, a significant deviation from linearity only occurred in the range of a 5-to-10-fold excess, indicating that intercalation at multiple sites in the 19-mer was supported at room temperature. Binding of TO to the external portions of DNA is also known to occur at sufficiently high concentrations [53, 54]. The data between Figs. 6 and 7 also show that the quenching efficiency is greater with TAMRA-ssDNA conjugates than TAMRA-dsDNA conjugates, suggesting that intercalation is favoured in the competition

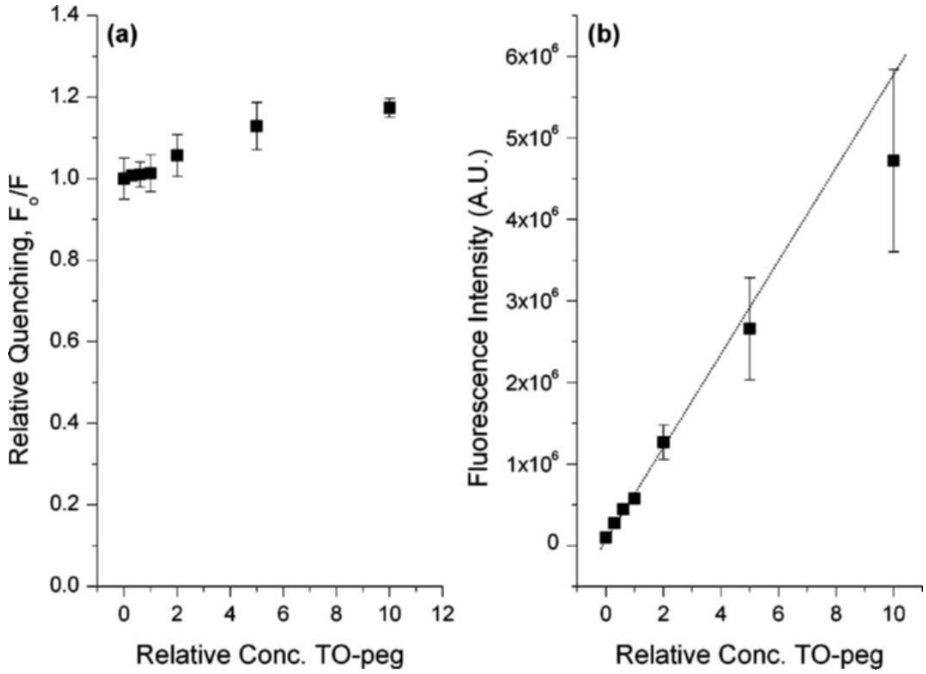

Fig. 7 (a) Quenching of TAMRA-dsDNA fluorescence as a function of the relative concentration of TO-alkyl. A linear fit has not been applied due to the competition between intercalation and complex formation. (b) TO fluorescence as a function of TO:dsDNA (unlabelled) ratio. The linear fit is applied to the ratios below 2:1. The concentration of dsDNA in each case is 0.4 μM

between intercalation and complex formation. Note also that the increase in TAMRA fluorescence at less than two equivalents of TO is also absent. This is consistent with our aforementioned hypothesis since we expect the nature of the dsDNA to dominate the local environment around TAMRA. In this sense, weak association of TO with the TAMRA or polyanionic backbone of the DNA would not significantly alter the environment of the TAMRA. There was another point of interest in this analysis in that the deviation from linearity of TO-dsDNA fluorescence that is seen in Fig. 6 at 5- and 10-fold excesses of TO represent changes of 10 and 19%, respectively. The quenching efficiencies of TO with TAMRA-dsDNA at these concentrations are 13 and 17%, respectively. While it could be suggested that this similarity indicates that complex formation occurred once the intercalative capacity of the 19-mer had been satisfied, this is not the case. Quenching was observed at TO concentrations in which intercalation retained its linearity, thus indicating that there was likely a competition between the two processes.

In light of this data, a FRET-based methodology for biosensor development which employs intercalating dyes must be carefully designed. The interaction of TO with TAMRA—particularly at stoichiometric excesses of the former—has the potential to be detrimental to the sensitivity of a sensor. It is clear that assays employing TO in the presence of a second dye should avoid large excesses of the former. In addition, it would be very worthwhile to tether a single TO molecule to the probe sequence at the terminus opposite the TAMRA label. Our data suggests that a tether which allows intercalation near the middle of the sequence (for oligonucleotides similar in size to those used in this work) would be effective in allowing FRET and preventing complex formation.

In addition to TO-TAMRA complex formation, we note that TO-TO dimerization can also occur at high concentrations of the dye. The dimerization of TO is well characterized in the literature [14, 55], and here we note that the onset of dimerization is a function of the side chain modification on the TO, i.e. hydrophobicity. With the more soluble (in aqueous buffer) TO-PEG, it was found that dimer formation became appreciable in the range of 10–15 μM. Using the less soluble TO-alkyl, it was found that dimer formation was appreciable even as low as 8 μM. The dimerization process is marked by the growth of a second absorption peak on the blue side of the monomeric TO absorption peak. The spectra we have obtained (data not shown) are in good agreement with those reported elsewhere [14, 54].

Conclusions

It has been demonstrated that TO is capable acting as a FRET donor for the acceptor dyes Cy3, TAMRA, IabFQ, Cy5, and IabRQ as dsDNA conjugates. Both fluorescence intensity and fluorescence lifetime data suggest a FRET mechanism, and the Förster distances for these pairs have been derived from experimental data. Furthermore, fluorescence lifetime data indicates that TO intercalates near the center of the double-stranded 19mer oligonucleotide that was used in this study. Discrepancies between the FRET efficiency derived from intensity and lifetime data are attributed to the ability of TAMRA-labelled oligonucleotide to form a non-fluorescent complex with TO. Complex formation has been investigated using polyethylene glycol and alkyl side chains attached to TO, and the results indicate greater fluorescence quenching with the more hydrophobic alkyl side chain. In addition, TO-TO dimerization was also found to be more extensive when using the more hydrophobic alkyl side-chain. These results indicate that combinations of dyes, or use of large quantities of a single dye with hydrophobic tendencies, must be carefully evaluated to avoid induction of associations between dyes. Physical associations may affect photophysical properties and lead to discrepancies in assay results that are anticipated from FRET. With respect to this last point, we have proposed and evaluated a variety of FRET schemes employing TO for the transduction of DNA hybridization events. It is found that a roughly four-fold increase in signal-to-noise ratio over a conventional TO-based assay can be obtained by using IabFQ to suppress background fluorescence from non-intercalated TO. Similarly, a proposed ratiometric scheme using TAMRA as a fluorescent acceptor dye is expected to yield a greater than five-fold increase in signal-to-noise ratio.

Acknowledgements We are grateful to Dr. Paul Piunno, Dr. Sergei Musikhin, and Dr. Arkady Major for their assistance in acquiring fluorescence lifetimes. In addition, we thank NSERC for financial support of this research work, and for provision of a research fellowship to WRA.

References

1. Almadidy A, Watterson J, Piunno PAE, Foulds IV, Horgen PA, Krull UJ (2003) A fibre-optic biosensor for detection of microbial contamination. Can J Chem/Rev Can Chim 81:339–349
2. Hartley HA, Baeumner AJ (2003) Biosensor for the specific detection of a single viable B-anthracis spore. Anal Bioanal Chem 376:319–327
3. Deisingh AK, Thompson M (2001) Sequences of E-Coli O157:H7 detected by a PCR-acoustic wave sensor combination. Analyst 126:2153–2158
4. Zhong XB, Reynolds R, Kidd JR, Kidd KK, Jenison R, Marlar RA, Ward DC (2003) Single-nucleotide polymorphism genotyping on optical thin-film biosensor chips. Proc Natl Acad Sci USA 100:11559–11564
5. Watterson JH, Raha S, Kotoris CC, Wust CC, Gharabaghi F, Jantzi SC, Haynes NK, Gendron NH, Krull UJ, Mackenzie AE, Piunno PAE (2004) Rapid detection of single nucleotide polymorphisms associated with spinal muscular atrophy by use of a reusable fibre-optic biosensor. Nucleic Acids Res 32:e18

6. Storri S, Santoni T, Mascini M (1998) A piezoelectric biosensor for DNA hybridization detection. Anal Lett 31:1795–1808
7. Xie H, Zhang CY, Gao ZQ (2004) Amperometric detection of nucleic acid at femtomolar levels with a nucleic acid/electrochemical activator bilayer on gold electrode. Anal Chem 76:1611–1617
8. Fojta M (2002) Electrochemical sensors for DNA interactions and damage. Electroanal 14:1449–1463
9. Mariotti E, Minunni M, Mascini M (2002) Surface plasmon resonance biosensor for genetically modified organisms detection. Anal Chim Acta 453:165–172
10. Rich RL, Myszka DG (2000) Survey of the 1999 surface plasmon resonance biosensor literature. J Mol Recognit 13:388–407
11. Lee M, Walt DR (2000) A fiber-optic microarray biosensor using aptamers as receptors. Anal Biochem 282:142–146
12. Haugland R (2002) Handbook of molecular probes and research products, 9th edn. Molecular Probes, Inc., Eugene
13. Rye HS, Yue S, Wemmer DE, Quesada MA, Haugland RP, Mathies RA, Glazer AN (1992) Stable fluorescent complexes of double-stranded DNA with bis-intercalating asymmetric cyanine dyes—properties and applications. Nucleic Acids Res 20:2803–2812
14. Nygren J, Svanvik N, Kubista M (1998) The interactions between the fluorescent dye thiazole orange and DNA. Biopolymers 46:39–51
15. Lee LG, Chen CH, Chiu LA (1986) Thiazole orange—A new dye for reticulocyte analysis. Cytometry 7:508–517
16. Kricka LJ (2002) Stains, labels, and detection strategies for nucleic acids assays. Ann Clin Biochem 39:114–129
17. Prodhomme S, Demaret J-P, Vinogradov S, Asseline U, Morin-Allory L, Vigny P (1999) A theoretical and experimental study of two thiazole orange derivatives with single- and double-stranded oligonucleotides. Polydeoxyribonucleotides and DNA. J Photochem Photobiol B 53:60–69
18. Norman DG, Grainger RJ, Uhrin D, Lilley DMJ (2000) Location of cyanine-3 on double-stranded DNA: Importance for fluorescence resonance energy transfer studies. Biochemistry 39:6317–6324
19. Valeur R (2002) Molecular fluorescence principles and applications. Wiley, VCH Verlag, GmbH, Weinheim
20. Wang X, Krull UJ (2005) Synthesis and fluorescence studies of thiazole orange tethered onto oligonucleotide: Development of a self-contained DNA biosensor on a fibre optic surface. Bioorg Med Chem Lett 15:1725–1729
21. Wang X, Krull UJ (2002) Tethered thiazole orange intercalating dye for development of fibre-optic nucleic acid biosensors. Anal Chim Acta 470:57–70
22. Nissum M, Jacobsen JP, Faurskov Nielsen O, Waage Jensen P (1997) Deterimination of the stability of complexes between DNA and the thiazole orange derivatives TO6 and TOTO by surface-enhanced resonance raman spectroscopy. Biospectr. 3: 207–213
23. Stærk D, Hamed AA, Pedersen EB, Jacobsen JP (1997) Bisintercalation of homodimeric thiazole orange dyes in DNA: Effect of modifying the linker. Bioconjug Chem 8:869–877
24. Laib S, Seeger S (2004) FRET studies of the interaction of dimeric cyanine dyes with DNA. J Fluoresc 14:187–191
25. Bordelon JA, Feierabend KJ, Siddiqui SA, Wright LL, Petty JT (2006) Viscometry and atomic force microscopy studies of the interactions of a dimeric cyanine dye with DNA. Phys J Chem B 106:4838–4843
26. Privat E, Asseline U (2001) Synthesis and binding properties of oligo-2′-deoxyribonucleotides covalently linked to a thiazole orange derivative. Bioconjug Chem 12:757–769
27. Privat E, Melvin T, Mérola F, Schweizer G, Prodhomme S, Asseline U, Vigny P (2002) Fluorescent properties of oligonucleotide-conjugated thiazole orange probes. Photochem Photobiol 75:201–210
28. Benson SC, Singh P, Glazer AN (1993) Heterodimeric DNA-binding dyes designed for energy-transfer-synthesis and spectroscopic properties. Nucleic Acids Res 21:5727–5735
29. Le Pecq JB, Paoletti C (1967) A fluorescent complex between ethidium bromide and nucleic acids—physical–chemical characterization. J Mol Biol 29:87–106
30. Hyun K-M, Choi S-D, Lee S, Kim SK (1997) Can energy transfer be an indicator for DNA intercalation? Biochim Biophys Acta 1334:312–316
31. Rye HS, Quesada MA, Peck K, Mathies RA, Glazer AN (1991) High-sensitivity 2-colour detection of double-stranded DNA with a confocal fluorescence gel scanner using ethidium homodimer and thiazole orange. Nucleic Acids Res 19:327–333
32. Laib S, Seeger S (2004) FRET studies of the interaction of dimeric cyanine dyes with DNA. J Fluoresc 14:187–191
33. Petty TJ, Bordelon JA, Robertson ME (2000) Thermodynamic characterization of the assocation of cyanine dyes with DNA. J Phys Chem B 104:7221–7227
34. Bunkenborg J, Gadjev NI, Deligeorgiev T, Jacobsen JP (2000) Concerted intercalation and minor groove recognition of DNA by a homodimeric thiazole orange dye. Bioconjug Chem 11:861–867
35. Bunkenborg J, Stidsen MM, Jacobsen JP (1999) On the sequence selective bis-intercalation of a homodimeric thiazole orange dye in DNA. Biconjug Chem 10:824–831
36. Rye HS, Glazer AN (1995) Interaction of dimeric intercalating dyes with single-stranded DNA. Nucleic Acids Res 23:1215–1222
37. Brooker LGS, White FL, Keyes GH, Smyth CP, Oesper PF (1941) Colour and constitution. II. Absorptions of some related vinylene-homologous series. J Am Chem Soc 63:3192–3203
38. Brooker LGS, Keyes GH, Williams WW (1942) Colour and constitution. V. The absorption of unsymmetrical cyanines. Resonance as a basis for a classification of dyes. J Am Chem Soc 63:199–210
39. Carreon JR, Mahon KP, Kelley SO (2004) Thiazole orange-peptide conjugates: Sensitivity of DNA binding to chemical structure. Org Lett 6:517–519
40. Koizumi M, Deitrich-Buchecker C, Sauvage JP (2004) A [2]catenane containing 1,1′-binaphthyl units and 1,10-phenanthroline fragments: Synthesis and intermolecular energy transfer processes. Eur J Org Chem 4:770–775
41. Cheung HC (1991) In: Lakowicz JR (ed) Topics in fluorescence spectroscopy, vol 2. Principles. Plenum, New York, pp 127–176
42. Sjöback R, Nygren J, Kubista M (1995) Absorption and fluorescence properties of fluorescein. Spectrochim Acta A 51:L7–L21
43. Massey M, Algar WR, Krull UJ (2006) Fluorescence resonance energy transfer (FRET) for DNA biosensors: FRET pair and förster distances for various dye-DNA conjugates. Anal Chim Acta (in press) DOI: 10.1016/j.aca.2005.12.050
44. Rasnik I, Mckinney SA, Ha T (2005) Surfaces and orientations: Much to FRET about? Acc Chem Res 38:542–548
45. Shins JM, Agronskaia A, de Grooth BG, Greve J (1999) Orientation of the chromophore dipoles in the TOTO-DNA system. Cytometry 37:230–237
46. Mizukami S, Kikuchi K, Higuchi T, Urano Y, Mashima T, Tsuruo T, Nagano T (1999) Imaging of capase-3 activation in HeLa cells stimulated with etoposide using a novel fluorescent probe. FEBS Lett 453:356–360
47. Daugherty DL, Gellman SH (1999) A fluorescence assay for leucine zipper dimerization: Avoiding unintended consequences of fluorophore attachment. J Am Chem Soc 121:4325–4333
48. West W, Pearce S (1965) Dimeric state of cyanine dyes. J Phys Chem 69:1894–1903
49. Geoghegan KF, Rosner PJ, Hoth LR (2000) Dye-pair reporter systems for protein-peptide molecular interactions. Bioconjug Chem 11:71–77
50. Valdes-Aguilera O, Neckers DC (1989) Aggregation phenomena in xanthene dyes. Acc Chem Res 22:171–177

51. Kikuchi K, Takakusa H, Nagano T (2004) Recent advances in the design of small molecule-based FRET sensors for cell biology. TrAC—Trends Anal Chem 23:407–415
52. Lakowicz JR (1999) Principles of fluorescence spectroscopy. Kluwer Academic/Plenum Publishers, New York
53. Larsson A, Carlsson C, Jonsson M, Albinnson N (1994) Characterization of the binding of the fluorescent dyes YO and YOYO to DNA by polarized-light spectroscopy. J Am Chem Soc 116:8459–8465
54. Larsson A, Carlsson C, Jonsson M (1995) Characterization of the binding of YO to Poly(DA-DT)] (2) and [Poly(DG-DC)] (2), and of the fluorescent properties of YO and YOYO complexed with the polynucleotides and double-stranded DNA. Biopolymers 36:153–167
55. Nygren J, Andrade JM, Kubista M (1996) Characterization of a single sample by combining thermodynamic and spectroscopic information in spectral analysis. Anal Chem 68:1706–1710